

Towards a compact THz local oscillator based on a quantum-cascade laser

H. Richter¹⁾, M. Greiner-Bär¹⁾, S. G. Pavlov¹⁾, A. D. Semenov¹⁾, M. Wienold²⁾, L. Schrottke²⁾,
M. Giehler²⁾, R. Hey²⁾, H. T. Grahn²⁾, and H.-W. Hübers^{1),3)}

¹⁾Institute of Planetary Research, German Aerospace Center (DLR), Rutherfordstr. 2,
12489 Berlin, Germany

²⁾Paul-Drude-Institut für Festkörperelektronik, Hausvogteiplatz 5–7, 10117 Berlin, Germany

³⁾Institut für Optik und Atomare Physik, Technische Universität Berlin, Hardenbergstraße 36,
10623 Berlin, Germany

ABSTRACT

Heterodyne spectroscopy of molecular rotational lines and atomic fine-structure lines is a powerful tool in astronomy and planetary research. One example is the OI fine-structure line at 4.7 THz. This is a main target to be observed with GREAT, the German Receiver for Astronomy at Terahertz Frequencies, which will be operated on board of SOFIA. We report on the development of a compact, easy-to-use source, which combines a quantum-cascade laser (QCL) a compact, low-input-power Stirling cooler. This work is part of the local-oscillator development for GREAT/SOFIA. The QCL, which is based on a two-miniband design, has been developed for high output and low electrical pump power. Efficient carrier injection is achieved by resonant longitudinal-optical phonon scattering. The amount of generated heat complies with the cooling capacity of the Stirling cooler. The whole system weighs less than 15 kg including cooler, power supplies etc. The output power is above 1 mW. With an appropriate optical beam shaping, the emission profile of the laser becomes a fundamental Gaussian one. Sub-MHz frequency accuracy can be achieved by locking the emission of the QCL to a molecular resonance. We will present the performance of the QCL-based source along with some application examples in high-resolution molecular spectroscopy.

1. INTRODUCTION

The terahertz (THz) portion of the electromagnetic spectrum bears an amazing scientific potential in astronomy and atmospheric research. Many fundamental absorption and emission lines of astrophysical and atmospheric important molecules and atoms occur in this spectral region. Up to now more than one hundred molecules and atoms have been detected in space. There are fairly simple molecules such as CO but also molecules consisting of ten or more atoms have been identified. High resolution spectroscopy in particular heterodyne spectroscopy of molecular rotational lines and fine structure lines of atoms or ions is a powerful tool which allows obtaining valuable information about the observed object such as temperature and dynamical processes as well as density and distribution of particular species.

A consortium consisting of the Max-Planck-Institute for Radioastronomy, the University of Cologne, the Max-Planck-Institute for Aeronomy, and the DLR in Berlin is currently developing the *German Receiver for Astronomy at Terahertz Frequencies* (GREAT).^{1,2} In the framework of this consortium DLR is responsible for the development of the high frequency channel which is aimed to cover selected frequencies between 3 THz and 5 THz. The main target is the fine structure line of neutral atomic oxygen, OI, at 4.74 THz. It is a major coolant line of the interstellar medium and is strongly emitted from the peripheries of interstellar clouds, where molecules such as CO or OH are photo-dissociated by interstellar UV radiation.

Typically, below ~2 THz multiplied microwave sources are used as local oscillator (LO). State of the art sources deliver as much as 20 μ W power at 1.8 THz.³ Above ~2 THz optically pumped gas lasers are used. They are relatively bulky and, more important, not tunable in frequency.⁴ THz quantum-cascade lasers (QCLs) are a promising alternative.⁵ The lasing mechanism is based on intersubband transitions in the conduction band of heterostructures, most commonly made from GaAs/AlGaAs. QCLs have several advantages over other sources. In particular, they are small, frequency tunable,

and require low electrical input power. Because liquid-helium cooling or cooling with bulky cryocoolers⁶ requiring large electrical power this is impractical for air- and spaceborne or commercial applications.

Here we report on the development of a compact, easy-to-use, continuous wave (cw) THz source, which is based on a QCL integrated in a compact, low-input-power Stirling cooler with a nominal cooling capacity of 7 W at 65 K. As a first step towards a QCL-based LO we have developed a QCL operating at 3.1 THz. Emphasis was put on optimizing the QCL for high output and low electrical pump power. This allows integrating the laser into a compact Stirling cooler. In a second step a laser operating at approximately 4.7 THz was developed and integrated into a Stirling cooler.

2. EXPERIMENTAL SETUP

The QCL was developed for an output power of several mW, cw operation at temperatures above 50 K, and an operating frequency of 3.1 THz. The pumping power is kept sufficiently low for integration into the Stirling cooler at the same time. The active region of the QCL consists of 85 periods with each period containing nine GaAs quantum wells and nine $\text{Al}_{0.15}\text{Ga}_{0.85}\text{As}$ barriers [6] and is sandwiched between a 700-nm-thick, Si-doped ($2 \times 10^{18} \text{ cm}^{-3}$) GaAs bottom contact layer and a 80-nm-thick, highly Si-doped ($5 \times 10^{18} \text{ cm}^{-3}$) top contact layer. The complete structure was grown by molecular-beam epitaxy on a semi-insulating GaAs(100) substrate. The two Si-doped layers form a single-plasmon (SP) waveguide. The active region is based on a two-miniband design, in which efficient injection into the upper laser level is achieved by an intersubband transition resonant to the energy of the longitudinal optical phonon. The operating electrical field strength lies between 5 and 6 kV/cm, which is about half the value for the conventional designs that are based on scattering of electrons on longitudinal optical phonons. The low operating voltage and the low current density (about several hundred A/cm^2) guarantee pumping powers below 7 W for the employed laser with a 100- μm -wide, 11- μm -thick, and 1.43-mm-long ridge. The design was optimized in such a way that a sufficiently large calculated gain was obtained with values above 50 cm^{-1} over a rather wide range of field strengths around 5 kV/cm. The electrical contacts are wire-bonded to the top layer and to both sides of the laser ridge. The chip with the QCL was soldered with indium on a gold-plated copper submount. The laser has a Fabry-Pérot cavity with both facets uncoated. A more detailed description of the QCL is given in Ref. [7]. The current for the QCL was supplied by a home-made, battery-driven current source.

The QCL is integrated into a commercial miniature cryocooler (model K535 from Ricor). This is a twin-piston, linear-integrated Stirling cooler operating with a 45 Hz cycle, which is dynamically balanced in order to minimize mechanical vibrations. The cooler has a nominal cooling capacity of 7 W at 65 K for an ambient temperature of 23 °C. It weighs 9.5 kg and has the dimensions $32.1 \times 13.9 \times 27.4 \text{ cm}^3$ (length \times width \times height). The power supply for the cooler unit weighs 2.6 kg and has the dimensions $10.2 \times 13.0 \times 33.6 \text{ cm}^3$. The average electrical input power measured over five hours continuous operation was 220 W. It is cooled with tap water at a flow rate between 1 and 4 l/min.

The submount with the QCL is attached to a second copper mount, which in turn is fixed to the cold finger of the Stirling cooler. In order to ensure tight thermal contacts, indium foil is placed between the two copper mounts as well as between the second copper mount and the cold finger. The temperature is measured with a Si diode thermometer installed close to the QCL submount. Variations induced by the 45 Hz operation cycle are less than 0.1 K. As expected, the Fourier spectrum of the temperature variations exhibits a peak at 45 Hz. Higher harmonics were not observed. Cold finger, copper mounts, and the QCL are encapsulated in a vacuum housing. Prior to operation, the housing is evacuated to a pressure of less than 1 Pa. The output window is made from z-cut quartz. In order to avoid standing waves and to minimize Fabry-Pérot type etalon effects in the setup and back reflections into the laser, the output window is somewhat tilted with respect to the optical axis. When the QCL is turned off, the cooler reaches its minimum temperature of 24 K approximately 25 min after it is switched on.

3. SYSTEM PERFORMANCE

Figure 1 shows the current-voltage and the light-current characteristics measured with a Golay cell detector. The starting temperature of 24 K increased to 43 K during measurement due to the increased power dissipation. The lowest operating temperature for the QCL emission that can be achieved with the Stirling cooler is approximately 35 K. At this temperature, the lasing threshold occurs at 300 mA and 6 V which corresponds to an electrical input power of 1.8 W and a threshold current density of 210 A/cm^2 . The output power is maximal in the range from 600 to 650 mA (approximately

5.0 to 5.8 W electrical input power). The maximal output power is 8 mW measured with a Thomas Keating opto-acoustic power meter in front of the vacuum window of the cooler. The steps in the output power are probably caused by electric-field domains, which can occur in doped or photoexcited semiconductor superlattices.⁸

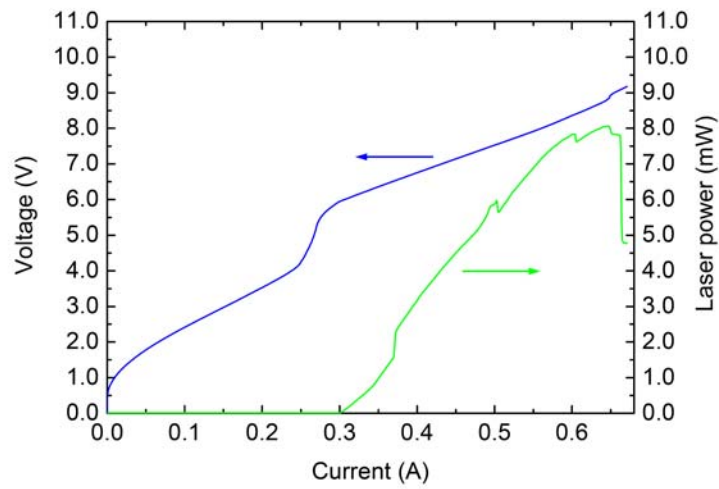


Figure 1. Voltage and output power of the QCL as a function of current. The steps in the output power are probably caused by electric-field domains.

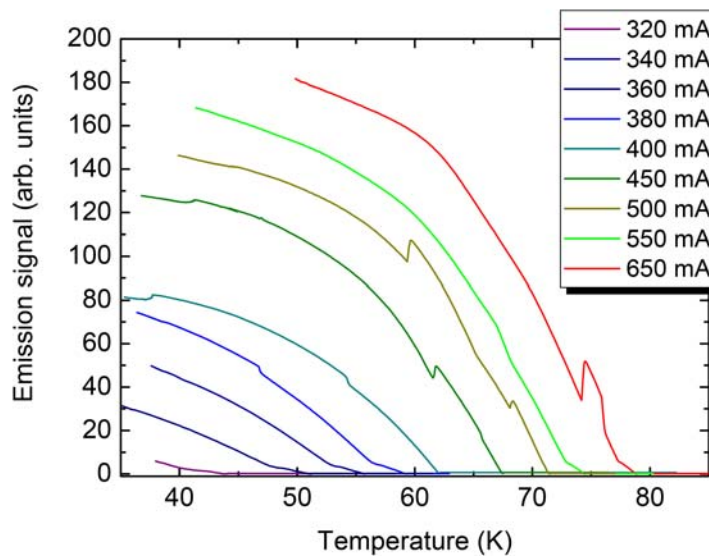


Figure 2. Laser output signal (cw) as a function of temperature for several driving currents.

The output power as a function of temperature for several driving currents is shown in Fig. 2. The laser was first cooled to the lowest operating temperature. Then the Stirling cooler was switched off, and the output power was measured as a function of temperature with a liquid-helium-cooled Ge:Ga photoconductive detector. A clear increase of the output power and maximum operating temperature is observed for increasing current values up to 650 mA. In this regime, the increase of the laser gain apparently overcompensates the thermally induced losses inside the laser.

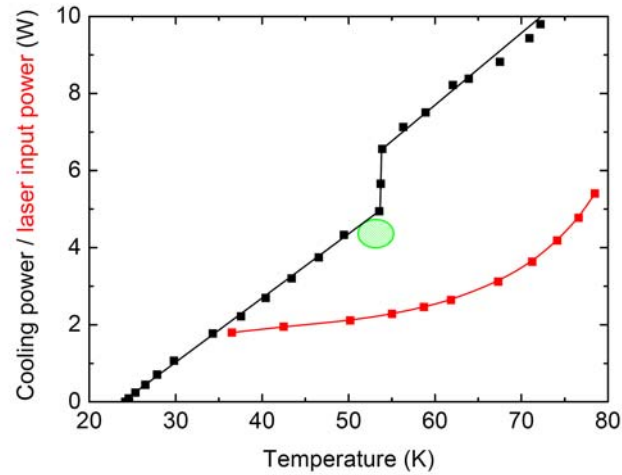


Figure 3. Electrical input power at lasing threshold of the QCL (red curve) and cooling power available from the Stirling cooler (black curve) as a function of temperature. The step at 54 K occurs because the internal temperature stabilization of the cooler does not function below this temperature. Across the whole range, the electrical input power at the temperature threshold is much less than the available cooling power. The green ellipse indicates the region of maximum output power.

The electrical input power at lasing threshold is plotted as a function of temperature along with the cooling power available from the Stirling cooler in Fig. 3. The step at 54 K is due to the internal temperature stabilization of the cooler which does not function below this temperature so that a stable operation mode with less cooling power prevents damage to the cooler. The cooling power was measured by resistive heating of the cold finger. Across the whole temperature range, the electrical input power at laser threshold is much less than the available cooling power. Laser operation stops at 78.6 K where the cooling power is still above the electrical input power. This indicates that the laser operation terminates for intrinsic reasons rather than due to a limited cooling capacity. The highest operating temperature is slightly above the boiling point of liquid nitrogen (77.4 K) so that operation with approximately 200 μ W output power is expected at this temperature. For a current value of 650 mA, a constant temperature of 52 K is reached after 15 min of laser operation.

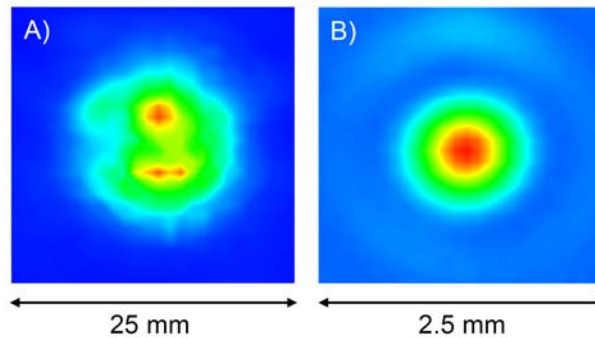


Figure 4. Beam profiles of the QCL. (a) Beam profile measured at 2.5 cm distance from the QCL. Two emission maxima (red) can be distinguished. One originates directly from the laser ridge, and the other one comes from the substrate. (b) Beam profile at the position of the minimum waist created by a lens in front of the QCL. The waist size is (0.7 ± 0.01) mm.¹¹

Fig. 4(a) shows the beam profile of the QCL measured by scanning a Golay cell detector with an aperture of 1 mm diameter in a plane orthogonal to the emission direction of the QCL at 2.5 cm distance. Two emission lobes can be

distinguished. The upper one is almost circular, while the lower one has an elongated, slightly curved shape. These lobes can be attributed to emission from the substrate, into which part of the laser mode extends, and from the active medium itself as has been shown in previous publications.^{9, 10} Besides the main lobes, there is a ring-like structure in the beam pattern. This is most probably caused by diffraction at the TPX lens. Although the surrounding of the back facet and parts of the copper submount were covered with non-transmitting material, there might be some residual reflections, which also contribute to the interference structure.

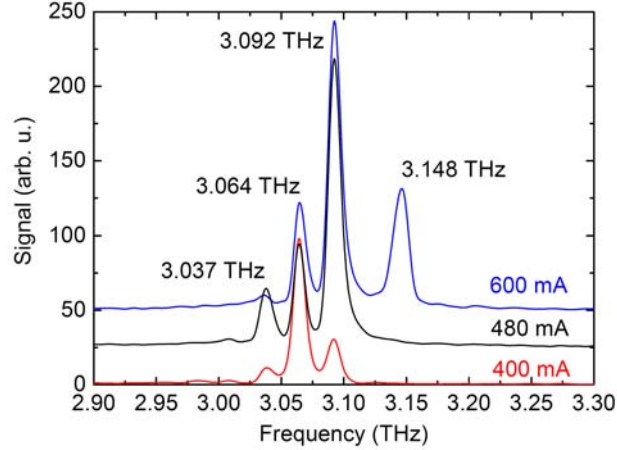


Figure 5. Emission spectra of the QCL measured with a Fourier transform spectrometer for 400, 480, and 600 mA at 39, 44, and 52 K, respectively. The spectral resolution is approximately 10 GHz. The spectra are shifted for clarity. Several longitudinal modes of the Fabry-Pérot laser cavity separated by 28 GHz appear. The frequency coverage is approximately 250 GHz.

The emission spectrum of the QCL was measured with a Fourier transform spectrometer. A liquid-helium-cooled Ge:Ga photoconductive detector was used and three spectra for 400, 480, and 600 mA at 39, 44, and 52 K, respectively, were measured (Fig. 5). The spectral resolution is approximately 10 GHz. Several emission peaks are observed, which are separated by 28 GHz covering a range of approximately 250 GHz. These are the longitudinal modes of the Fabry-Pérot laser cavity. Their frequency separation is given by $\Delta\nu = c/(2n_{\text{eff}} L)$, with c denoting the speed of light, n_{eff} the effective refractive index of the active medium, and L the length of the laser cavity. With $\Delta\nu = 28$ GHz and $L = 1.43$ mm, this yields $n_{\text{eff}} = 3.75$. Within the spectral resolution, none of the modes exhibits any frequency shift. The lack of any measureable frequency shift indicates a tunability of less than 50 MHz/mA. With increasing current, the output power increases, more modes appear, and the modes at higher frequencies become more intense relative to the lower frequency ones. This is probably caused by two optical transitions involved in the lasing process and a change in the relative population of the two emitting subbands.⁷

4. TOWARD HIGH-RESOLUTION SPECTROSCOPY

As a first demonstration of the capability of the compact QCL source for spectroscopic applications, the absorption of $^{12}\text{CH}_3\text{OH}$ was measured with high spectral resolution around 3.1 THz. The experiment was performed by changing the current of the QCL and detecting the laser emission after transmission through an absorption cell. In this way, the laser frequency of each mode can be tuned over a spectral region of less than 10 GHz. The experimental setup is shown in Fig.6.

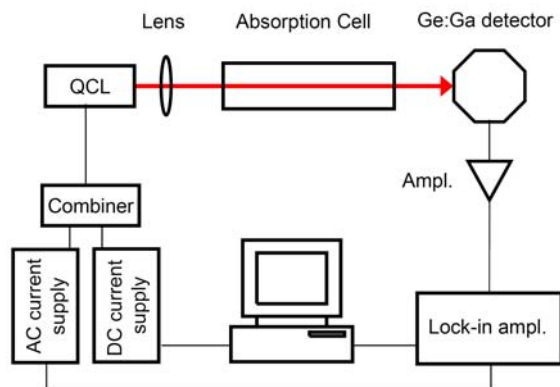


Figure 6. Experimental set-up for gas-phase spectroscopy.

The diverging QCL beam was focused with the same TPX lens as for the imaging experiment through a 52-cm-long absorption cell onto a Ge:Ga detector, which was followed by a low-noise amplifier. The vacuum windows of the cell were tilted in order to avoid standing waves. The cell was filled with $^{12}\text{CH}_3\text{OH}$ at a pressure of 4.4 hPa measured with a capacitive manometer. The current of the QCL was modulated at a frequency of 10 kHz with a peak-to-peak amplitude of 1.6 mA by superposition of the modulation current from a frequency synthesizer with a DC current. The output signal from the low-noise amplifier was detected with a lock-in amplifier using the 10 kHz current modulation as a reference and an integration time of 1 ms. This results in a derivative-like absorption signal.

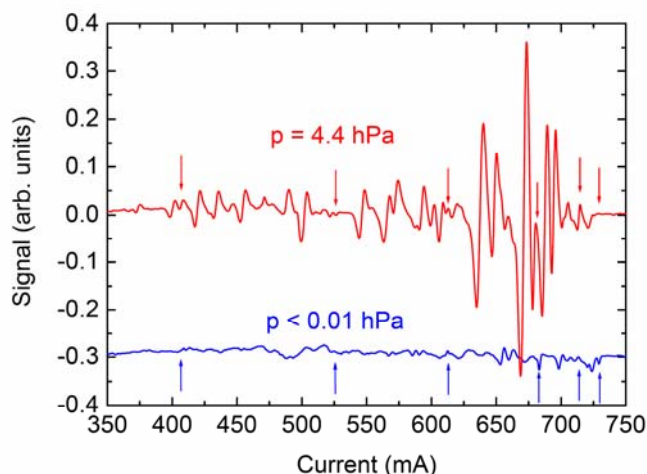


Figure 7. Absorption signal of $^{12}\text{CH}_3\text{OH}$ as a function of laser current at 53 K for 4.4 hPa (red curve) and below 0.01 hPa (black curve). The black curve is shifted by 0.3 for clarity. Each scan took only 320 ms. The maximum signal-to-noise ratio is 1500.

As an example, the absorption signal is shown in Fig. 7 as a function of the laser current for pressures of 4.4 hPa and < 0.01 hPa. The recording time for the whole spectrum amounted to only 320 ms. At 4.4 hPa, absorption signals appear across the whole range of QCL drive current. The lock-in detection yielded a signal-to-noise ratio, which is as large as 1500 despite the short measurement time. The rather complicated absorption structure is due to the multimode operation of the laser, because each mode generates its own spectrum. The FWHM of the absorption lines has been determined from the corresponding derivative-like signals¹⁵. It is approximately 4 mA. Although the pressure broadening coefficients of these particular absorption lines have not been reported in the literature, it is reasonable to assume that they are about the same as for other methanol transitions¹². Therefore, we can expect a FWHM of about 100 MHz at

4.4 hPa. This indicates a frequency tunability of around 25 MHz/mA in agreement with the upper limit established by the Fourier transform spectra.

5. TOWARDS A 4.7-THZ LOCAL OSCILLATOR FOR GREAT/SOFIA

After the demonstration of the principal performance characteristics of the 3.1-THz QCL in a compact Stirling cooler a QCL for 4.7 THz was made. It is 100- μm -wide, 11- μm -thick, has a 1-mm-long ridge and a Fabry-Pérot cavity with both facets uncoated. The QCL was mounted in a Stirling cooler system similar to the system described above, but with air cooling instead of water cooling. In Fig. 8 a photograph of the Stirling cooler with the vacuum housing for the QCL is shown. The performance of the Stirling cooler is identical to the one described in the previous sections. With this system a cw output power of $\sim 50 \mu\text{W}$ has been achieved.

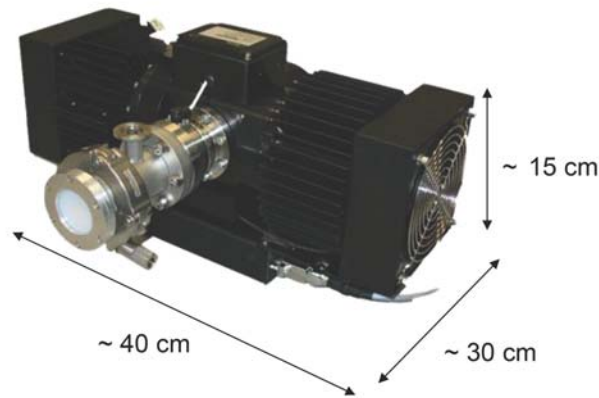


Figure 8. Aircooled Stirling cooler system. It weighs 9.5 kg and the average electrical input power measured over five hours continuous operation is $\sim 220 \text{ W}$.

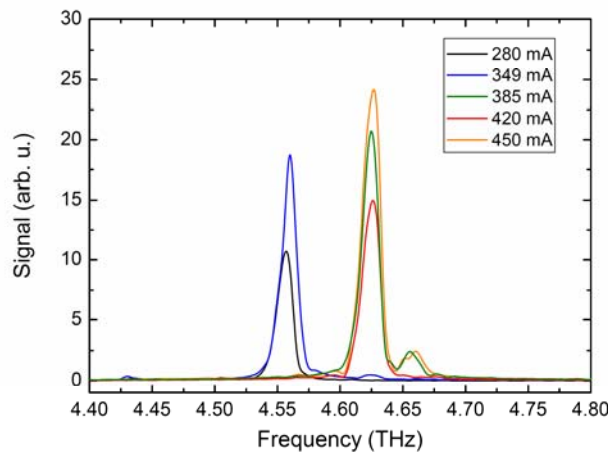


Figure 9. FTS spectrum of the first QCL designed for 4.7 THz. The temperature during operation was 30 K.

The FTS spectrum is shown in Fig. 9. As can be seen the first design and manufacturing approach has resulted in a gain profile which is approximately at the correct frequency. The gain maximum is approximately 100 GHz ($\approx 2\%$) too low.

The next steps will be to adjust the gain medium to 4.7 THz, to use a distributed feedback (DFB) grating in order to yield monomode operation, and a frequency stabilization with a gas cell.¹⁵

A possible way to implement this system into GREAT/SOFIA is shown in Fig. 10. The system is compatible with the mass, volume, and power restrictions of GREAT/SOFIA.

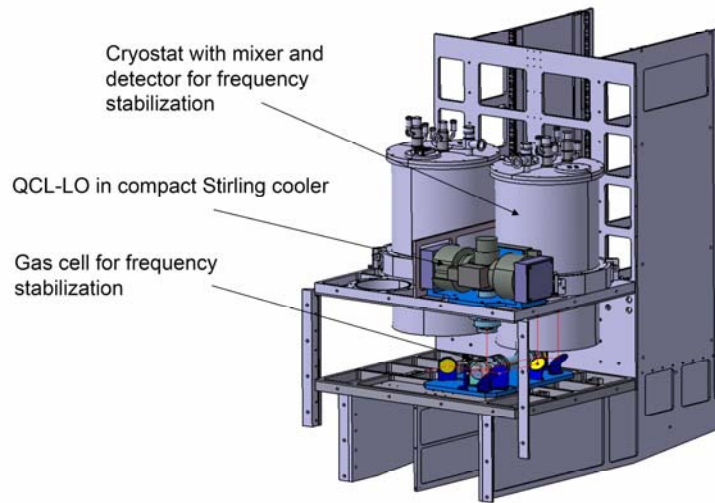


Figure 10. Possible implementation of the compact 4.7 THz source in the GREAT/SOFIA system. The system is compatible with the mass, volume, and power restrictions of GREAT/SOFIA.

6. SUMMARY AND CONCLUSION

We have realized a compact, cw THz source based on a QCL and a miniature cryocooler. The broad frequency coverage of almost 10% of the emission frequency makes it attractive for implementation into an external cavity which will allow for tuning of the emission frequency across a broad range as required for a spectrometer. Furthermore, the water-cooled Stirling cooler, which was used because it was readily available, was replaced by an air-cooled instrument, which provides the same cooling capacity as the water-cooled one. This cooler was used to make measurements of a QCL designed for 4.7 THz. Along with frequency stabilization by for example locking to an external reference such as the emission from a multiplied microwave source or to a molecular absorption line, this source is an attractive option for a THz local oscillator.^{13,14,15}

REFERENCES

- [1] R. Güsten, P. Hartogh, H.-W. Hübers, U. U. Graf, K. Jacobs, H. P. Röser, F. Schäfer, R. T. Schieder, R. Stark, J. Stutzki, P. van der Wal, and A. Wunsch, "GREAT: The First Generation German Heterodyne Receiver for SOFIA", in: *Airborne Telescope Systems*, ed. by R. K. Melugin and H. P. Röser, *Proc. SPIE* **4014**, 23 (2000).
- [2] R. Güsten, P. Hartogh, H.-W. Hübers, U. U. Graf, K. Jacobs, C. Kasemann, H.-P. Röser, R. T. Schieder, G. Schneider, O. Siebertz, J. Stutzki, G. Villanueva, A. Wagner, P. Van der Wal, and A. Wunsch, "GREAT: The German Receiver for Astronomy at Terahertz Frequencies", in: *Airborne Telescope Systems*, ed. by R. K. Melugin and H. P. Röser, *Proc. SPIE* **4857**, 56 (2002).
- [3] I. Mehdi, "THz local oscillator technology", in *Millimeter and Submillimeter Detectors for Astronomy II*, J. Zmuidzinas, W. S. Holland, and S. Withington, eds., *Proc. SPIE* **5498**, 103-112 (2004).

- [4] H.-W. Hübers, A. Semenov, H. Richter, M. Schwarz, B. Günther, K. Smirnov, G. Gol'tsman, and B. Voronov, "Heterodyne Receiver for 3-5 THz with Hot Electron Bolometric Mixer", in: *Millimeter and Submillimeter Detectors for Astronomy II*, J. Zmuidzinas, W. S. Holland, and S. Withington, eds., *Proc. SPIE* **5498**, 579-586 (2004).
- [5] R. Köhler, A. Tredicucci, F. Beltram, H. E. Beere, E. H. Linfield, A. G. Davies, D. A. Ritchie, R. C. Iotti, F. Rossi, "Terahertz semiconductor-heterostructure laser", *Nature* **417**, 156-159 (2002).
- [6] H. Richter, A. D. Semenov, S. G. Pavlov, L. Mahler, A. Tredicucci, H. E. Beere, D. A. Ritchie, K. S. Il'in, M. Siegel, and H.-W. Hübers, "Terahertz heterodyne receiver with quantum cascade laser and hot electron bolometer mixer in a pulse tube cooler", *Appl. Phys. Lett.* **93**, 141108 (2008).
- [7] M. Wienold, L. Schrottke, M. Giehler, R. Hey, W. Anders, and H. T. Grahn, "Low-voltage terahertz quantum-cascade lasers based on LO-phonon-assisted interminiband transitions", *Electron. Lett.* **45**, 1030-1031 (2009).
- [8] L. L. Bonilla and H. T. Grahn, "Nonlinear dynamics of semiconductor superlattices", *Rep. Prog. Phys.* **68**, 577-683 (2005).
- [9] H.-W. Hübers, S. G. Pavlov, A. D. Semenov, R. Köhler, L. Mahler, A. Tredicucci, H. E. Beere, D. A. Ritchie, and E. H. Linfield, "Terahertz quantum cascade laser as local oscillator in a heterodyne receiver", *Opt. Express* **13**, 5890-5896 (2005).
- [10] E. Bründermann, M. Havenith, G. Scalari, M. Giovannini, J. Faist, J. Kunsch, L. Mechold, and M. Abraham, "Turn-key, compact high temperature terahertz quantum cascade lasers: imaging and room temperature detection", *Opt. Express* **14**, 1829-1841 (2006).
- [11] H. Richter, M. Greiner-Bär, S. G. Pavlov, A. D. Semenov, M. Wienold, L. Schrottke, M. Giehler, R. Hey, H. T. Grahn, and H.-W. Hübers, "A compact, continuous-wave terahertz source based on a quantum-cascade laser and a miniature cryocooler", *Opt. Express* **10177**, Vol. 18, No. 10, (2010).
- [12] H.-W. Hübers, S. G. Pavlov, H. Richter, A. D. Semenov, L. Mahler, A. Tredicucci, H. E. Beere, and D. A. Ritchie, "High-resolution gas phase spectroscopy with a distributed feedback terahertz quantum cascade laser", *Appl. Phys. Lett.* **89**, 061115 (2006).
- [13] D. Rabanus, U. U. Graf, M. Philipp, O. Ricken, J. Stutzki, B. Vowinkel, M. C. Wiedner, C. Walther, M. Fischer, and J. Faist, "Phase locking of a 1.5 Terahertz quantum cascade laser and use as a local oscillator in a heterodyne HEB receiver", *Opt. Express* **17**, 1159-1168 (2009).
- [14] P. Khosropanah, A. Baryshev, W. Zhang, W. Jellema, J. N. Hovenier, J. R. Gao, T. M. Klapwijk, D. G. Paveliev, B. S. Williams, Q. Hu, J. L. Reno, B. Klein, and J. L. Hesler, "Phase locking of a 2.7 THz quantum cascade laser to a microwave reference", *Opt. Letters* **19**, 2958-2960 (2009).
- [15] H. Richter, S. G. Pavlov, A. D. Semenov, L. Mahler, A. Tredicucci, H. E. Beere, D. A. Ritchie, and H.-W. Hübers, "Sub-megahertz frequency stabilization of a terahertz quantum cascade laser to a molecular absorption line", *Appl. Phys. Lett.* **96**, 071112 (2010).